ULTRASONIC RAYLEIGH WAVE ENHANCEMENTS FROM ANGLED DEFECTS IN ALUMINIUM

A.R. Clough, B. Dutton, R.S. Edwards.

Department of Physics, University of Warwick, Coventry, UK

ABSTRACT. Non-linear enhancements of ultrasonic surface wave amplitude and frequency have been observed when an incident wave interacts with a surface defect. Previous measurements of surface wave interactions with defects have considered only those that are inclined normal to the surface. Here, the enhancement effects have been studied in aluminium samples with machined slots of fixed length and of varying angle to the horizontal; the degree of enhancement was studied as a function of defect angle using both a scanning laser source, and a scanning laser detector. An automated scanning system has been developed for use with the detector, an IOS two-wave mixer interferometer, capable of measuring the out-of-plane surface displacement on rough surfaces. B-scans, consisting of many A-scans stacked together, were used to identify wave modes present in the near field, the arrival times of which are dependent on the angle of the defect. The observed enhancement is caused by superposition of the incident Rayleigh wave with reflected and mode converted waves, thereby making it angle dependent.

Keywords: Ultrasound, Rayleigh Waves, Enhancement, Angled Defects
PACS: 81.70.Cv, 81.70.-q, 43.35.Zc, 43.20.Gp

INTRODUCTION

It is known that surface waves such as Rayleigh waves will interact with a surface defect, and measuring the properties of the transmitted and reflected waves can help to characterise the defect [1-4]. Furthermore, amplitude and frequency enhancements in the near field have been reported previously for a Rayleigh wave incident on a surface defect [3]. This previous work focussed on enhancements arising from defects normal to the sample surface [3,4,6], however, many industrial failures arise from defects that have grown at an angle to the surface. Rolling contact fatigue in rails, for example, commonly propagates at an angle of 25° to the sample surface, and stress corrosion cracking defects can propagate at any given angle to the surface. Both of these defects can cause costly damage to industrial components and can be very challenging to detect. The amplitude and frequency enhancement effects observed in the near field of these defects may be useful to characterise the angle of the defect, and subsequently the defect type, prior to catastrophic damage occurring.

For this work, ultrasonic waves are generated in aluminium samples which have machined surface defects set at various angles to the horizontal, using a pulsed Nd:YAG laser line source. Detection is via an Intelligent Optics Systems (IOS) two-wave mixer interferometer, which detects the out-of-plane surface displacement of the sample [9]. Both the laser detector and the laser source are scanned over the defect, and the near field behaviour for both of these measurements is studied as a function of the defect angle. High

resolution B-scans were formed over the course of each experiment, and several angle dependent wave modes were identified. Amplitude and frequency enhancements observed in the near field, caused by superposition of the incident Rayleigh wave and these reflected and mode converted waves, and / or through the changing boundary conditions near to the defect, were studied as a function of the defect angle, with a view to being able to predict the defect angle from enhancement data. Experimental data was compared to that obtained from PZFlex, a finite element method (FEM) simulation package.

THEORY

A Rayleigh wave incident on a surface defect can either be reflected, transmitted or mode converted due to scattering from the defect [1]. Previous work identified several mode converted longitudinal and shear waves produced by interaction with the defect, in samples with a machined defect perpendicular to the sample surface [4]. This work has been extended to cover mode conversion arising from defects set at various angles to the horizontal and has been verified both experimentally and through FEM simulations [5].

If the arrival times of any reflected and/or mode converted waves coincide with that of the incident Rayleigh wave, superposition of the waves will occur [6]. This leads to an increase in the peak to peak amplitude of the incident Rayleigh waves in the near field when the arrival times coincide due to constructive interference. The degree to which the Rayleigh wave is enhanced is dependent upon the arrival times, the reflection coefficient for the defect, and ultimately the angle of the defect relative to the surface. Previously we reported measurements of the reflection coefficient as a function of angle, and it is to be expected that this will have a significant effect on the enhancement [5,7]. The increased amplitude of the Rayleigh wave will subsequently lead to an increase in the frequency content at the Rayleigh wave peak frequency, and hence a simultaneous frequency enhancement is expected. This will enable a prediction of the defect angle from the observed enhancements, and will further aid in defect characterisation [3].

In the far field, the arrival times of the surface waves (Rayleigh, mode-converted surface skimming longitudinal) are dependent on the crack depth, but not the angle. However, the mode converted longitudinal and shear waves produced by scattering of the incident Rayleigh wave have arrival times that are dependent upon the angle of the defect that has caused the scattering [4,5]. It is important to understand this angle dependence as the mode-converted waves and possible wave-paths in the near-field may affect the signal enhancement measured. For shallow angled defects, this mode-conversion to bulk waves may also play a more important role than previously assumed.

The theoretical arrival times can be calculated for scanning the detection point over a defect using the following expressions [5]. In the following, x is defined to be the modulus of the distance of the laser detector to the defect, l is the distance of the laser source to the defect, θ is the angle of the defect relative to the surface and d is the length of the defect. The velocities of the Rayleigh, shear and longitudinal waves are $v_R = 2940$ ms^{-1}, $v_C = 6300$ ms^{-1} and $v_S = 3110$ ms^{-1} respectively. A subscript of r describes a reflected wave, while t relates to a wave that has been transmitted by the defect. The geometry of the defect is illustrated in figure 1.

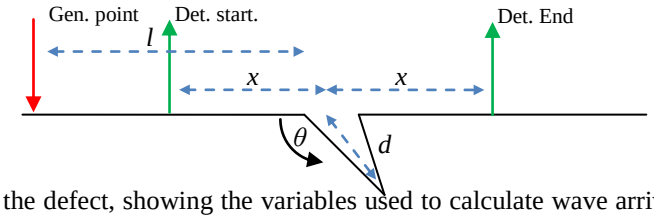

FIGURE 1. Geometry of the defect, showing the variables used to calculate wave arrival times and the fixed generation point, scanned detection point.

A Rayleigh wave (subscript R) incident on the defect can be reflected directly from the crack opening, or transmitted / reflected up and down the defect before the final reflection or transmission. The arrival time at the detection point of these waves is described by equation 1;

(1)

where k is an integer ≥ 0. For transmission the wave with $k = 0$ corresponds to a low frequency wave that penetrates beneath the defect. There is also the possibility of mode conversion to a longitudinal surface skimming wave (subscript C) at the defect opening; described by equation 2;

(2)

Mode conversion to both shear (S) and longitudinal (C) waves from the defect tip has also been reported [4], and a portion of these waves will reach the surface, their arrival times being dependent upon the defect angle. These are described by equations 3 – 6, where the subscript h denotes a wave that has been mode converted from the defect tip.

(3)

(4)

(5)

(6)

There exists a second set of angle dependent wave modes, which are generated via mode conversion at the bottom of the defect of the low frequency Rayleigh wave ($k = 0$) that penetrates under the defect. These are described by equations 7 – 10, where the subscript g denotes these as being generated by the $k = 0$ Rayleigh wave.

(7)

(8)

(9)

(10)

For the case of the laser source passing over the defect, not all of these mode-converted waves will be observed due to attenuation of the waves [1,4]. In this case, in the near field the contribution of the mode-converted surface skimming longitudinal wave, shown to be significant for the detection point over the defect, will be minimal [4]. However, the expected enhancement will not only be caused by superposition of waves but also by the changing conditions under which the ultrasound is being generated [3,6]. As the

source passes over the defect the portion of the surface that is illuminated changes, and the source profile will change [8]. As the energy transferred to the sample is dependent upon both the temporal and spatial features of the source, the altered beam profile changes the conditions and hence affects the behaviour of the ultrasound. More details can be found in references [3,6,8].

In addition to identifying the angle of the defect from the enhancement factors, the unique pattern of arrival times observed in experimental B-scans can be compared with knowledge of the expected arrival times of the mode converted waves in order to predict the defect angle. This is achieved through matching the observed arrival times with the expected times until a satisfactory agreement is observed. To this date, this has only been achieved through visual inspection by a trained operator; however a system is under development to create a program capable of identifying the defect angle from the B-scan data.

EXPERIMENTAL METHODS

Experimental Setup

The defects studied were laser micro machined v–shaped defects with a constant length *d* of 2mm, across the entire width of a face of each aluminium sample (see figure 1). The samples were held in place and the detection and generation lasers were passed over the defect. A fixed separation was maintained between the two lasers during the experiments so that the degree of attenuation of the incident Rayleigh wave experienced across a scan was the same at each detection point. The laser source was a 1064 nm Nd:YAG laser focussed to a line source of approximate dimensions 6 mm by 300 μm, operating in the thermoelastic regime to avoid damage to the sample [8]. The IOS system has a detection point of approximately 200 μm in diameter, and no surface preparation was carried out on the sample [9]. For the detector point passing over the defect, scans are labelled as scanned laser detector (SLD), while for the generation laser passing over the defect scans are labelled scanned laser source (SLS), following reference [6].

Finite Element Method

FEM models were produced with the same geometry as the experimental setup, with a dipole force used to simulate the laser line source, and detection carried out along the centre line of the defect in the case of SLD [5,7]. In the SLS models a thermal source was used, so that the generation conditions would be correct when the generation laser directly illuminated the defect. Models were carried out for a range of defect angles, from 20° to 160°, and with varying defect depths. The depth to wavelength ratio (d/λ) ranged from 0.14 to 1.33, and these models were used as an aid to understanding the experimental results. In order to avoid lengthy calculations involved with changing the generation position in SLD experiments, the separation between detector and generator was allowed to change; this is illustrated by the different gradient of the incident Rayleigh wave in figure 2.

RESULTS

A range of angled defects ($20° \leq \theta \leq 150°$) were studied using both SLD (detector moving over defect) and SLS (line source moving over defect) techniques. A series of A-scans were recorded in each case, which were then stacked together to produce an arrival

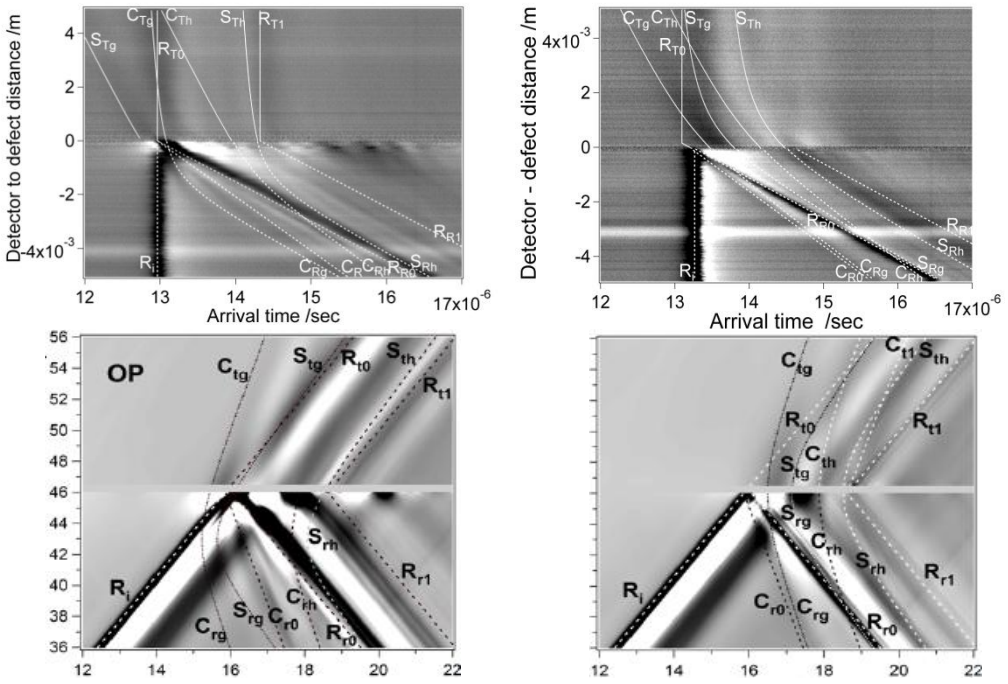

FIGURE 2. B-scans from experimental (top) and modelled (bottom) defects for defect angles of 40° (left) and 90° (right). Calculated arrival times have been superimposed on top of B-scans.

time B-scan. The expected arrival times for the mode converted waves were calculated and superimposed onto the B-scans using equations 1-10 in order to verify their existence. The equations were modified slightly for the experimental measurements in order to take into account the fixed-separation of the generation and detection points. The agreement between the theoretical and experimental arrival times was good, as seen in figure 2, where the top B-scans show the experimental data for a fixed separation, while the lower B-scans show the FEM results, where the generation point has been held fixed as in figure 1.

The amplitude enhancement factors were found by windowing each A-scan over the Rayleigh wave arrival time and measuring the peak to peak amplitude of the surface displacement, and identifying how it changed during a B-scan. At the point at which constructive interference between the incident Rayleigh wave and some reflected and mode converted waves occurred, an increase in the peak to peak amplitude was observed. The ratio between the enhanced peak amplitude and that observed far away from the defect was taken to be the amplitude enhancement factor for that specific angle [10]. Taking this ratio had the effect of normalising the incident Rayleigh wave amplitude between different samples, allowing the differing sample surface conditions to be taken into account. These amplitude enhancement factors were compared between the experimental data and the FEM data, and results are presented in figure 3.

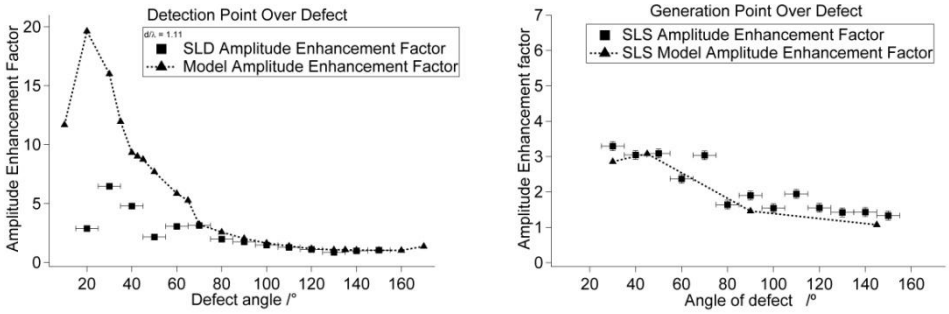

FIGURE 3. Amplitude enhancement factors as a function of angle for both modelled and experimental data, for SLD (left) and SLS (right).

For the SLD measurements, the difference in the magnitude of the amplitude enhancement factors between the experimental and FEM data arises from the fact that the simulation data is recorded at a very small point, whereas the experimental data is averaged over the physical spot size of the detector [10]. For these measurements the detection beam was not completely focussed and hence the averaged amplitude around the point at which maximum enhancement occurs is reduced. However, the general trend for the change in enhancement with angle is consistent, and it can be seen that the amplitude enhancement is more pronounced for angles of less than 90°, with the magnitude of the enhancement factor being approximately 1 for angles larger than 90° (i.e. no signal enhancement in the windowed Rayleigh wave arrival time). This reinforces the behaviour observed in the B-scans for angles higher than 90° shown in figure 2, where the reflected and mode-converted surface skimming longitudinal wavemodes from the crack opening are very small, and the arrival times of the mode-converted bulk waves are away from the windowed Rayleigh arrival time. This therefore verifies that the enhancement is caused largely by the constructive interference of various wave modes arriving simultaneously. For very small angles, a comparison of SLD and SLS experiments suggests that the more sensitive approach may be SLD, particularly when comparing the modelled data (lines in figure 3) and considering a smaller detection size.

Frequency B-scans were produced by windowing the A-scans about the incident Rayleigh wave and performing a fast Fourier transform (FFT), and using these to produce a B-scan of frequency content similar to the amplitude B-scan [3]. This produces the distinctive B-scans shown in figure 4, in which the position of the defect is clearly visible, and the differences caused by varying defect angle are also immediately obvious. Potential measurements can include tracking the frequency at which the FFT has its peak magnitude [6], or measuring this peak magnitude, which should change during the scan in a similar manner to the amplitude signals. In addition, the magnitude of the FFT at a higher frequency than the frequency content of the Rayleigh wave may give more information [3].

The peak FFT magnitude of the incident Rayleigh wave was tracked across the B-scan in a similar fashion to the peak to peak amplitude described above, and again a ratio of the enhanced value to that far away from the defect was used to produce a frequency enhancement factor. The behaviour of the frequency enhancement factors as a function of angle is shown in figure 5(a) for SLD and SLS measurements. As expected, this behaviour follows a pattern similar to the amplitude enhancement factor, again enabling the angle of the defect for $\theta \leq 90^{\circ}$ to be predicted from the observed enhancement factor. Again, the modelled FFT magnitude enhancements for SLD are larger than those measured, due to the finite size of the detection point.

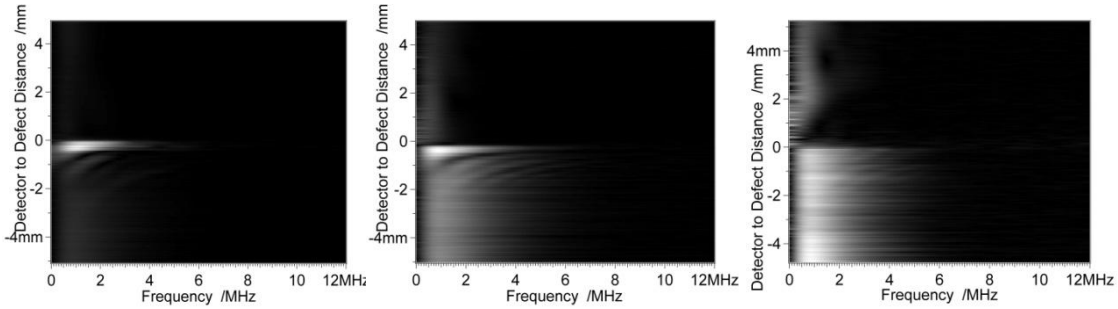

FIGURE 4. FFT B-scans for defects of 40˚ (left), 90˚ (centre) and 140˚ (right) to the surface. FFTs are carried out on the time window for the incident Rayleigh wave.

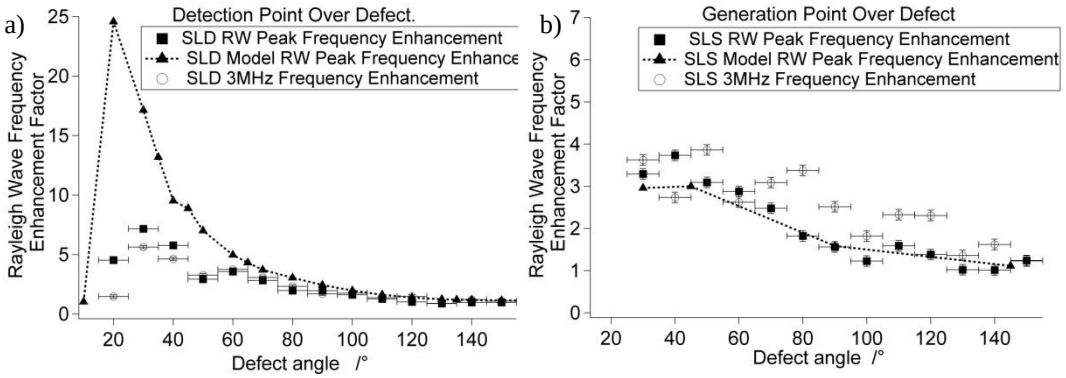

FIGURE 5. Frequency enhancement factors as a function of angle for both modelled and experimental data, with SLD (a) and SLS (b).

A method for identifying the defect position was also developed by looking at the frequency content of the received ultrasound at a given higher frequency, in this case 3 MHz. Far away from the defect the frequency content at 3 MHz is minimal as the peak frequency of the Rayleigh wave lies around 0.8 MHz, however, near the point at which enhancement occurs the frequency content at the higher frequencies increases dramatically for shallow angles, enabling the position of the defect to be accurately tracked by simply studying one frequency, provided that this frequency is suitably different to that of the incident Rayleigh wave [3]. Results are shown in figure 5(a) and (b), with the magnitude enhancement for both SLD and SLS being slightly higher at 3 MHz.

CONCLUSIONS

The method presented above enables the angle of the defect to the horizontal for smooth sided defects to be identified through two methods. The matching of the experimentally observed arrival times of mode converted waves to those predicted theoretically allows the angle of the defect to be characterised. This information can then be re-enforced through calculation of the amplitude and frequency enhancement factors, and used to definitively identify the defect angle, especially for those angles where $\theta \leq 90°$. For an angled defect, a scan in one direction may have an angle relative to the incident Rayleigh wave of > 90°, however, on changing over the generation and detection point the defect will have an angle of < 90°.

The defect position can also be determined accurately through examination of the data in the frequency domain. At the point at which enhancement occurs, a large increase in the magnitude of higher frequency components is observed, allowing the position of the defect to be found through examination of only one frequency. This allows for the simple determination of defect positions from data in which it may be difficult to clearly identify the defect position in the temporal domain. This will be particularly beneficial for shallow defects where the changes in arrival times caused by the defect are small, and hence the changes in the amplitude B-scan are minimal.

ACKNOWLEDGEMENTS

This work was funded by the European Research Council under grant 202735, ERC Starting Independent Researcher Grant.

REFERENCES

1. I.A. Viktorov. “Rayleigh and Lamb waves: physical theory and applications.” *Plenum Press* 1967.
2. B. Vu, V. Kinra. “Diffraction of Rayleigh waves in a half space. I. Normal edge crack.” *J. Acoust. Soc. Am*. 77 (4) April 1985.
3. S. Dixon, B. Cann, D.L. Carroll, Y. Fan and R.S. Edwards. “Non-linear enhancement of laser generation ultrasonic Rayleigh waves by cracks.” *Nondestructive Testing and Evaluation*. Vol. 23, No. 1, March 2008, 25 – 34.
4. X. Jian, S. Dixon, N. Guo and R.S. Edwards. “Rayleigh wave interaction with surface breaking cracks.” *J. Appl. Phys*. **101**, pp. 064906 (2007).
5. B. Dutton, A.R. Clough, M.H. Rosli and R.S. Edwards. “Non-contact ultrasonic detection of angled surface defects.” *Under review*.
6. A.K. Kromine, P.A. Fomitchov, S. Krishnaswamy, J.D. Achenbach. “Laser ultrasonic detection of surface breaking discontinuities: scanning laser source technique.” *Materials Evaluation*. February 2000, 173 – 177.
7. B. Dutton, R.S. Edwards, M.H. Rosli. “Defect feature extraction using surface wave interactions and time-frequency behaviour.” *Review of progress in quantitative non-destructive evaluation*. Feb. 22nd 2010. Vol 1211, pp. 647 – 654.
8. C.B. Scruby, L.E. Drain. “Laser ultrasonics: techniques and applications.” *Adam Hilger*, 1990.
9. M. Klien, G. Bacher, A. Grunnet-Jepson, D. Wright, W. Moerner. “Homodyne detection of ultrasonic surface displacements using two-wave mixing in photorefractive polymers.” *Optics communications*, 162 (1999) 79 – 84.
10. R.S. Edwards, X. Jian, S. Dixon. “Signal enhancement of the in-plane and out-of-plane Rayleigh wave components.” *Applied Physics Letters* **87**, 194104 (2005)